

# Algorithm for Simple Automated Breast MRI Deformation Modelling

Marta Danch-Wierzchowska, Damian Borys and Andrzej Swierniak

*Institute of Automatic Control, Silesian University of Technology, Akademicka 16, 44-100 Gliwice, Poland*

**Keywords:** Breast Deformation, Finite Element Modeling, MRI Images.

**Abstract:** Increasing incidence of breast cancer caused development of patient-specific treatment planning procedures. The most effective tool for breast cancer visualisation is Magnetic Resonance Imaging (MRI). However, the MRI scans represent patient data in prone position with breast placed in signal enhancement coils, while other procedures, i.e. surgery, PET-CT (Positron Emission Tomography fused with Computer Tomography) are performed in patient supine position. The bigger patient breast is, the bigger its shape differ in every patient position, what influences its interior structure and tumour location. In this paper, we present our method for automated breast model deformation, which is based on prone MRI dataset. Proposed algorithm allows to obtain reliable breast model in supine position in a few simple steps, without manual intervention.

## 1 INTRODUCTION

Recent studies show that breast cancer is the most frequent women's cancer around the world and it is the second most frequent among all human cancers. Due to that, diagnosis needs to be precise and fast, whereas treatment needs to be as personalised as possible. Therefore, breast tissue deformation has recently gained interest in various medical applications. Considering specific anatomy of the female breast any examination or intervention results in breast deformation. For that reason, on every examined image set the tumour in question is placed in different area. Moreover, female breast is very complex and irregular structure, consists of glandular lobules, adipose, milk ducts, connective tissues and skin. It is impossible to model glandular lobules and milk ducts as separate layers, since it is almost impossible to differentiate them on the MRI (Magnetic Resonance Imaging). Due to that, breast is usually modeled as four layers: fibroglandular, fat, skin and muscle (Han et al., 2012). In case of breast deformation modelling geometric transformation are mainly used for rigid and minor non-rigid deformation (i.e. respiratory movements) (Rueckert et al., 1999). To model major non-rigid deformation (i.e. mammography compression or prone to supine movement) knowledge-based transformation inspired by biomechanical models is used. FEM (Finite Element Modeling) is a numerical technique and, the same, allows approximate solving of partial differential equations (PDE), which simplifies

computations. The main motivation of biomechanical FEM models usage is that more information enables reliable estimation of complex deformation (Lee et al., 2010).

There are several applications of biomechanical breast modelling. Almost all of them are related to breast cancer diagnostics and treatment. The oldest praxis is a mammography simulation which presents the breast deformation caused by the plates compression (Han et al., 2012), (Pathmanathan et al., 2008). Another, more recent, application is breast deformation caused by the gravitational force. Such simulation is commonly used when different breasts shapes comparison is needed, e.g. MRI compared with PET-CT (Han et al., 2014). Fusion of different examinations helps with more accurate diagnosis (Abreu et al., 2013). Breast shape simulation in different patient positions is used in treatment planning and tumour location during medical procedures, e.g. surgery, biopsy procedure (Azar et al., 2000). Already published studies concentrate on creating one breast model based on patient or phantom data and its deformation with one or few methods. The results presented are very precise, but methodology impossible to be applied in a broader spectrum.

Different modalities of breast imaging are carried out in different patient positions. Especially, MRI imaging, the most powerful method nowadays, is acquired in patients lying in prone body position, with the breast hanging down into the coil. However, majority of therapeutic procedures, like surgery or radiation

therapy are carried out in supine body position, with significant displacement of breast tissue. Thus, the simple method of breast deformation modelling will be of clinical use, even if it is expected that the error of this modelling will not allow for ideal transposition of image. However, even rough transformation gives better estimation of tissue relationships than the routinely carried out visual assessment, regularly used in the clinic.

There appear some limitations that cause inaccuracies of the created models. The main issue is accurate tissue parameter estimation. Biomechanical properties of breast tissues have been measured *ex vivo* (A.Samani et al., 2007), (Wellman et al., 1999). However living tissues have different properties than those, extracted from body without blood circulation. Moreover existing *in vivo* measuring methods (i.e. elastography) do not provide information precise enough to estimate big deformation (Insana et al., 2005). Another issue is accurate mesh selection. Different types of mesh elements and different mesh node density give different results (Samani et al., 2001) and in some cases the FE mesh requires manual intervention (Han et al., 2012) as well as image segmentation (Han et al., 2014), (Pathmanathan et al., 2008). Further difficulty provides boundary conditions setting, especially on chest wall side, where the model ends but the real body consistency needs to be preserved (Tanner et al., 2002). Still unsolved modelling issue remains patient-specific, fully-automated image deformation algorithm, which is essential in clinical practice.

In this paper we present a basic idea of a simple breast model and its deformation, paying a special attention to further use in clinical practice. Presented paper is an extension to our previous work described in (Danch-Wierzchowska et al., 2016b). More precisely, previously presented algorithm was extended to 3D, so that image dataset is processed as one 3D object, instead of processing images one by one separately. The algorithm itself was modified to eliminate issues, that were not significant, nor present in 2D model. The biggest challenges were to determine dependencies between nodes and set model's boundary conditions and to preserve computational-time efficiency, while processing significantly bigger number of nodes, than in 2D analysis. In our work, we concentrated on simple and efficient way to model breast deformation, that would help with breast cancer diagnosis and could be used in clinical practice.

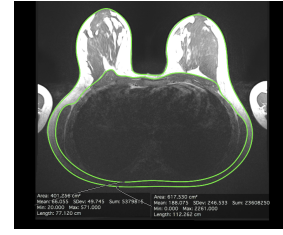


Figure 1: Exemplary breast MR image (internal green contour is a chestwall boundary, external green contour is a body boundary).

## 2 MATERIAL AND METHODS

### 2.1 Breast MRI Data Acquisition

MRI is widely used in medical diagnosis, in particular breast imaging (Behrens et al., 2007). It is safe technique because the MRI does not use the ionizing radiation. The possibility of multiple contrasts acquisitions, both anatomical and functional, plays a key role in MRI breast cancer detection. In this work we use T1-weighted MRI scans, which were acquired at the Center of Oncology ... with a Siemens scanner. The data consist of 50 axial slices of patient in prone position covering the area of interest. Obtained data cover approximately  $0.7 \times 0.7 \times 3$  mm real volume per voxel. Exemplary image, with Region of Interest (ROI) outlined in the Figure 1. The obtained MRI data constitutes basis for FEM construction. This method requires domain (image set) discretisation, tissue parameter estimation, transformation equation definition, boundary condition setting (see 2.2).

### 2.2 Deformation Algorithm

Deformation algorithm consist of a few main steps based on FEM best practices and is fully implemented in MATLAB.

**Breast Segmentation.** To obtain breast mask based on MRI image, a fuzzy c-means algorithm is used (Wu et al., 2013). However, after segmentation, manual correction is needed. The breast mask used in our algorithm is based on ROI presented in the Figure 1, but to the point of a widest diameter of a patient chest. Exemplary image mask is presented in the Figure 2.

**Dividing into Left/Right Part.** To shorten computational time, the model is divided into left and right

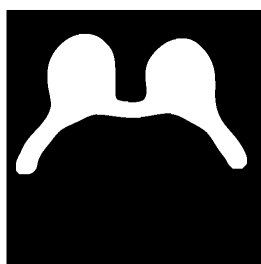


Figure 2: Exemplary breast MR image mask.

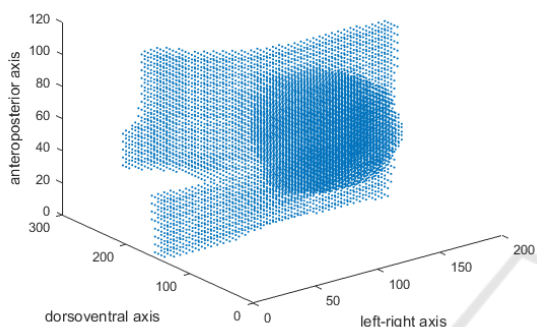


Figure 3: Exemplary resulting mesh for image set (one point represents one mesh node).

breast, which are joined in one model after deformation. Since there is no difference in methodology we present only one half of the model.

**Mesh Generation.** Mesh generation is a process where the coordinates of object domain nodes are set. In case of breast MRI transformation the mesh generation is performed in two steps: (1) - generating equidistant mesh for whole image set - domain volume, (2) - choosing nodes, which overlap a segmented images mask. The resulting mesh is presented in the Figure 3. For more details about mesh type see 4.

**Finding Boundary Nodes.** To set different parameters, the created model is divided into three parts (See Figure 4): skin nodes, chestwall nodes and other (fat and fibroglandular as one type) nodes. Boundary nodes are set using neighborhood dependencies and spatial localization.

**Setting Nodes Parameters.** Tissue parameters were set according to (Azar et al., 2002) as isotropic, homogeneous and incompressible material. Since the data was obtained from patients at age 50-70 with relatively big breast, it is justifiable to use simplification of the breast model based on assumption, that fat material parameters have much more influence on

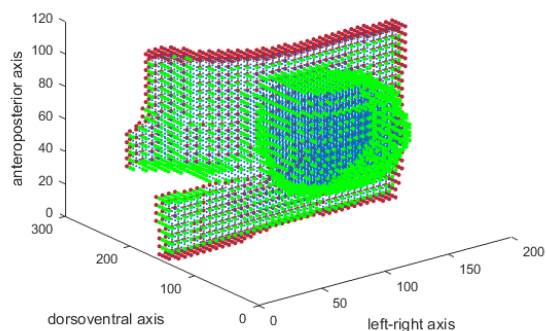


Figure 4: Boundary conditions for mesh, chestwall nodes (red), skin nodes (green).

deformation than fibroglandular ones (Pathmanathan et al., 2008). Skin nodes constrain collision detection and reaction. Chestwall nodes are set as stationary. However, their material parameters are set, to simulate breast tissues sliding along muscles. Material parameters used in the algorithm are presented in the Table 1.

Table 1: Model parameters.

Node type	Young Modulus	Poission's ratio
Skin	101 kPa	0.4995
Chestwall	5 kPa	0.1
Other	50 kPa	0.48

**Incorporation of Gravitational Force.** To implement deformation model (Azar et al., 2002) simplified Lagrange equation of motion was used. The gravitational force is applied to every node (except chestwall nodes) in the mesh. Displacement of each node is iteratively calculated according to implemented equation of motion. For more details see 4.

The incorporation of the gravitational force in the model is performed in two steps: (1) Removal of the gravitational force resulting from prone patient position, (2) Application of gravitational force resulting from supine patient position.

### 3 RESULTS

The exemplary deformation result is presented as breast mesh in the supine plan. Figure 5 shows selected mesh stages for an image set. The left image is the original mesh, the middle is stage (1) of deformation - unload model (See 2.2), while the right image contains the resulting mesh in supine patient position. The resulting mesh was compared with ANSYS model created for the same patient in our previous work (Danch-Wierzchowska et al., 2016a) (See

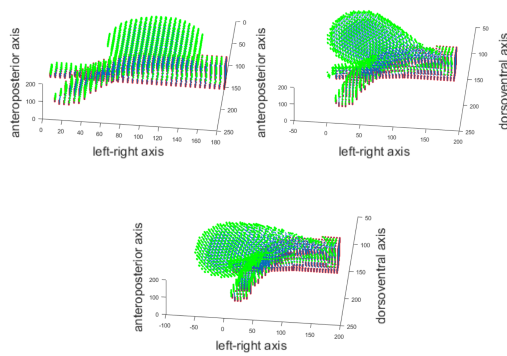


Figure 5: Selected mesh deformation stages: original mesh (upper left), unload mesh (upper right), resulting mesh (bottom), (green - skin nodes, red - stiffened nodes, blue - other nodes).

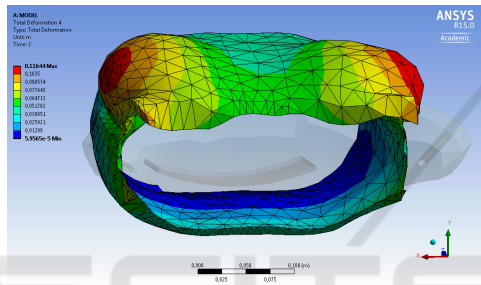


Figure 6: Reference ANSYS model (Danch-Wierzchowska et al., 2016a).

Figure 6). Differences are easily visible. However, the main shape is preserved.

Presented results are obtained in less than 30 min per dataset on average portable computer, with mostly automated algorithm. The only part, that requires manual correction and extend computation time is the image segmentation. This allows us to believe, that our algorithm, optimised and improved, would be useful in clinical practice.

## 4 DISCUSSION AND CONCLUSIONS

It is clear that results obtained could not be precise. There are many more conditions influencing tissue movement than the gravitational force. There is still muscle tension, which influences breast shape. It is impossible to mimic all body dependencies and movements personalized for every patient in limited time. However, there are image processing algorithms, like free-form deformation (FFD), which were successfully used for small non-linear deformation (Rueckert et al., 1999). The FFD algorithm could help

with a precise fitting of MRI image to supine reference image. Such images are obtained during PET-CT for example, which is also common practice in breast cancer diagnosis. Unfortunately, FFD is inefficient for large image deformations and cannot be used as the only deformation tool.

In our previous work we have presented two different approaches to breast deformation modelling. In (Danch-Wierzchowska et al., 2016a) we created a simplified woman's chest model and simulate prone to supine position changing in ANSYS. This work was focused on tumour displacement while patient position changing. The modelling error of tumour displacement was less than 2 cm for approx. 1cm tumour diameter and the results were deemed useful by collaborating physicians. However, working with ANSYS required too much effort to be used in everyday clinical practice. Moreover, costs of license and training are too expensive for average medical unit. Our second approach (Danch-Wierzchowska et al., 2016b) was based on one image deformation, i.e. only 2D deformation model was required. Obtained results were comparable with the result obtained with ANSYS model. The 2D results were compared with referenced, cross-section images from ANSYS model. The 3D algorithm presented in this paper eliminates the main cause of inaccuracy in 2D modelling by adding movement in anteroposterior axis and maintains tissue continuity in every direction. Nevertheless it is not free from inaccuracy yet and needs further improvement.

Modelling of breast deformation is mainly focused on the impact of gravitational force on the breast shape. One of the main challenges is a compromise between model accuracy and efficiency. Complex tissue models, representing every type of tissue, present in the breast as separate layer (Han et al., 2012), could never be used in clinical practice, since adapting them to each patient would be too time-consuming. To represent real breast movement several types of constitutive models were created. Most popular way to describe stress-strain relationship for fat and glandular tissue is the hyperelastic neo-Hookean constitutive model (Hopp et al., 2012). Analysis using available commercial software (i.e. ANSYS) gives acceptable results and allows to use complex constitutive tissue models, but implementing a body geometry inside it is still highly time-consuming (Danch-Wierzchowska et al., 2016a), (Han et al., 2012). The best solution would be to create a fully automated algorithm, which builds geometry based directly on medical images and deforms it, without using any third-party software, especially when using it requires manual cooperation. The model should be based only on breast essential



structures chosen as a compromise between accuracy and efficiency. Developing a fully-automated tool for creating a simplified model and incorporating gravitational force will speed up the image analysis significantly, along with time of diagnosis.

Our results show, that it is possible to create a simple model and in a few steps to deform it in a way useful for treatment planning. Our main goal was to mimic body displacement in the smallest possible number of steps with automated procedure, and it is clear that the results obtained have a limited precision. We concluded, that there is no need to use more sophisticated tissue constitutive model. Since the simplest one gives acceptable results, preserving computational efficiency, there is no purpose in complicating the model. At the moment the methodology does not require exact numerical Performance Index, since the shape differences are easily visible. However, with such simple tissue model and simple deformation equation, the results are promising. Improving the deformation algorithm, creating MRI images from obtained deformed mesh and proper segmentation methods will be under further investigation of our work.

## ACKNOWLEDGEMENTS

This work was supported by the Polish National Center of Research and Development grant no. STRATEGMED2/267398/4/NCBR/2015 (MILESTONE - Molecular diagnostics and imaging in individualized therapy for breast, thyroid and prostate cancer) (AS, DB) and the Institute of Automatic Control, Silesian University of Technology under Grant No. BKM-508/RAU1/2017/t.1 (MDW).

## REFERENCES

- Abreu, F. D., Wells, W., and Tsongalis, G. (2013). The emerging role of the molecular diagnostics laboratory in breast cancer personalized medicine. *Am J Pathol.*, 183(4):1075–83.
- A.Samani, Zubovits, J., and Plewes, D. (2007). Elastic moduli of normal and pathological human breast tissues: an inversion-technique-based investigation of 169 samples. *Phys Med Biol.*, 52(6):1565–76.
- Azar, F., Metaxas, D., and Schnall, M. (2000). A finite element model of the breast for predicting mechanical deformations during biopsy procedures. *Proceedings of the IEEE Workshop on Mathematical Methods in Biomedical Image Analysis*, pages 38–45.
- Azar, F., Metaxas, D., and Schnall, M. (2002). Methods for modelling predicting mechanical deformations of the breast under external perturbations. *Med Image Anal.*, 6:1–27.
- Behrens, S., Laue, H., Althaus, M., Boehler, T., Kuemmerlen, B., Hahn, H., and Peitgen, H. (2007). Computer assistance for MR based diagnosis of breast cancer: present and future challenges. *Comput Med Imaging Graph.*, 31(4-5):236–247.
- Danch-Wierzchowska, M., Borys, D., Bobek-Billewicz, B., Jarzab, M., and Swierniak, A. (2016a). Simplification of breast deformation modelling to support breast cancer treatment planning. *Biocybernetics and Biomedical Engineering*, 36(4):531–536.
- Danch-Wierzchowska, M., Borys, D., and Swierniak, A. (2016b). Breast deformation modeling based on mri images, preliminary results. *Information Technologies in Medicine*, 472:227–234.
- Golub, G. and Welsch, J. (1969). Calculation of gauss quadrature rules. *Mathematics of Computation*, 23(106):221–230.
- Han, L., Hipwell, J., Eiben, B., Barratt, D., Modat, M., Ourselin, S., and Hawkes, D. (2014). A nonlinear biomechanical model based registration method for aligning prone and supine MR breast images. *IEEE Trans Med Imaging.*, 33(3):682–94.
- Han, L., Hipwell, J., Tanner, C., Taylor, Z., Mertzani, D., Cardoso, J., Ourselin, S., and Hawkes, D. (2012). Development of patient specific biomechanical models for predicting large breast deformation. *Phys Med Biol.*, 57:455–472.
- Hopp, T., Dietzel, M., Baltzer, P., Kreisel, P., Kaiser, W., Gemmeke, H., and Ruiter, N. (2012). Automatic multimodal 2D/3D breast image registration using biomechanical FEM models and intensity-based optimization. *Med Image Anal.*, 17(2):209–218.
- Insana, M., Liu, J., Sridhar, M., and Pellot-Barakat, C. (2005). Ultrasonic mechanical relaxation imaging and the material science of breast cancer. *IEEE Ultrasonics Symposium*.
- Kattan, P. (2008). *MATLAB Guide to Finite Elements, An Interactive Approach*. Second edition, Springer-Verlag, Berlin, Heidelberg.
- Lee, A., Schnabel, J., Rajagopal, V., Nielsen, P., and Nash, M. (2010). Breast image registration by combining finite elements and free-form deformations. *Digital Mammography Lecture Notes in Computer Science*, (6136):736–743.
- Pathmanathan, P., Gavaghan, D., Whiteley, J., Chapman, S., and Brady, J. (2008). Predicting tumor location by modeling the deformation of the breast. *IEEE Trans Biomed Eng.*, 55(10):2471–80.
- Rueckert, D., Sonoda, L., Hayes, C., Hill, D., Leach, M., and Hawkes, D. (1999). Nonrigid registration using free-form deformations: application to breast mr images. *IEEE Trans Med Imaging*, 18(8):712–21.
- Samani, A., Bishop, J., Yaffe, M., and Plewes, D. (2001). Biomechanical 3-d finite element modeling of the human breast using mri data. *IEEE Trans Med Imaging.*, 20(4):271–9.
- Tanner, C., Schnabel, J., Smith, A., Sonoda, L., Hill, D., Hawkes, D., Degenhard, A., Hayes, C., Leach, M.,

and Hose, D. (2002). The comparison of biomechanical breast models: initial results. *ANSYS Convergence*.

Wellman, P., Howe, R., Dalton, E., and Kern, K. (1999). Breast tissue stiffness in compression is correlated to histological diagnosis. *Journal of Biomechanics*, (40)17745).

Wu, S., Weinstein, S., Conant, E., Schnall, M., and Kontos, D. (2013). Automated chest wall line detection for whole-breast segmentation in sagittal breast MR images. *Med. Phys.*, 40(4)(042301).

## APPENDIX

### Discretisation of the Domain

First step in the finite element analysis is object domain discretisation - division into smaller domain elements. It replaces the body with infinite degrees of freedom by a finite number of elements with finite and strictly defined degrees of freedom.

For three dimensional analysis one can discriminate two main type of elements: four node tetrahedral element (T4) and eight node hexahedral element (Q8). In this paper we focus on Q8 - linear brick element. The Q8 element described in local coordinates ( $\xi$ ,  $\eta$ ,  $\mu$ ) is presented below. (See Figure 7).

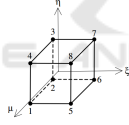


Figure 7: Linear brick element in local coordinates (Kattan, 2008).

### Basic Equations in FEM Elastic Deformation

The linear brick element is described by eight shape functions listed as follows in terms of local  $\xi$ ,  $\eta$  and  $\mu$  coordinates:

$$\begin{aligned} N_1 &= \frac{1}{8}(1-\xi)(1-\eta)(1+\mu), \\ N_2 &= \frac{1}{8}(1-\xi)(1-\eta)(1-\mu), \\ N_3 &= \frac{1}{8}(1-\xi)(1+\eta)(1-\mu), \\ N_4 &= \frac{1}{8}(1-\xi)(1+\eta)(1+\mu), \\ N_5 &= \frac{1}{8}(1+\xi)(1-\eta)(1+\mu), \\ N_6 &= \frac{1}{8}(1+\xi)(1-\eta)(1-\mu), \\ N_7 &= \frac{1}{8}(1+\xi)(1+\eta)(1-\mu), \\ N_8 &= \frac{1}{8}(1+\xi)(1+\eta)(1+\mu), \end{aligned} \quad (1)$$

The strain displacement matrix is described as follows:

$$B = \frac{1}{|J|} [B_1 B_2 B_3 B_4 B_5 B_6 B_7 B_8], \quad (2)$$

Table 2: Point coordinates and weights for two points Gauss-Legendre quadrature.

n	$\xi_i = \eta_i = \mu_i$	$W_i$
2	$\xi_1 = \xi_2 = \xi_3 = \pm 0.577350269189626$	$W_1 = W_2 = W_3 = 1$

where  $J$  is the Jacobian determinant and the nodal  $B_i$  matrix is given by:

$$B_i = \begin{bmatrix} \frac{\partial N_i}{\partial x} & 0 & 0 \\ 0 & \frac{\partial N_i}{\partial y} & 0 \\ 0 & 0 & \frac{\partial N_i}{\partial z} \\ \frac{\partial N_i}{\partial y} & \frac{\partial N_i}{\partial x} & 0 \\ 0 & \frac{\partial N_i}{\partial z} & \frac{\partial N_i}{\partial y} \\ \frac{\partial N_i}{\partial z} & 0 & \frac{\partial N_i}{\partial x} \end{bmatrix}. \quad (3)$$

Element plane strain matrix is given as follows:

$$D = \frac{E}{(1+\nu)(1-2\nu)} \begin{bmatrix} 1-\nu & \nu & \nu & 0 & 0 & 0 \\ \nu & 1-\nu & \nu & 0 & 0 & 0 \\ \nu & \nu & 1-\nu & 0 & 0 & 0 \\ 0 & 0 & 0 & \frac{1-2\nu}{2} & 0 & 0 \\ 0 & 0 & 0 & 0 & \frac{1-2\nu}{2} & 0 \\ 0 & 0 & 0 & 0 & 0 & \frac{1-2\nu}{2} \end{bmatrix}. \quad (4)$$

with Young Modulus  $E$  and Poisson's ratio  $\nu$ .

The element stiffness matrix is given by:

$$k = \int_{-1}^1 \int_{-1}^1 \int_{-1}^1 B^T D B J d\xi d\eta d\mu. \quad (5)$$

Two points Gauss-Legendre quadrature (Golub and Welsch, 1969) is used for practical evaluation of integrals (5) over the element volume. The point coordinates and weights are presented in the Table 2.

To calculate nodal displacement the following structural equation is used:

$$U = F K^{-1}, \quad (6)$$

where  $U$  is a node displacement matrix,  $F$  is nodal forces matrix and  $K$  is a global stiffness matrix. Once the boundary conditions are set, matrix  $U$  is solved by partitioning and Gaussian elimination. For more details see (Kattan, 2008).